Changes in optical conductivity due to readjustments in the electronic density of states

Mei-Rong Li[1] and J. P. Carbotte[2]
[1]*Department of Physics, University of Guelph, Guelph, Ontario, Canada N1G 2W1*
[2]*Department of Physics and Astronomy, McMaster University, Hamilton, Ontario, Canada L8S 4M1*
(Received 25 January 2002; revised manuscript received 5 July 2002; published 24 October 2002)

Within the model of elastic impurity scattering, we study how changes in the energy dependence of the electronic density of states (EDOS) $N(\epsilon)$ around the Fermi energy ϵ_F are reflected in the frequency-dependent optical conductivity $\sigma(\omega)$. While conserving the total number of states in $N(\epsilon)$ we compute the induced changes in $\sigma(\omega)$ as a function of ω and in the corresponding optical scattering rate $1/\tau_{\rm op}(\omega)$. These quantities mirror some aspects of the EDOS changes but the relationship is not direct. Conservation of optical oscillator strength is found not to hold, and there is no sum rule on the optical scattering rate although one does hold for the quasiparticle scattering. Temperature as well as increases in impurity scattering leads to additional changes in optical properties not seen in the constant EDOS case. These effects have their origin in an averaging of the EDOS around the Fermi energy ϵ_F on an energy scale set by the impurity scattering.

DOI: 10.1103/PhysRevB.66.155114 PACS number(s): 78.20.Bh

I. INTRODUCTION

Measurements of the infrared conductivity $\sigma(\omega)$ as a function of energy ω continue to give valuable information on charge dynamics in a wide range of metallic systems including the high-T_c superconducting cuprates.[1,2] These materials have received a lot of recent attention because they represent strongly correlated systems which exhibit new physics, beyond the usual Fermi liquid (FL) description of electric structure. It was recognized and emphasized as crucial very early on that the normal-state properties of the cuprates are anomalous. A marginal Fermi liquid[3–5] (MFL) phenomenology was developed which could describe remarkably well many of the observed deviation from FL behavior of the normal state. An essential feature of the MFL is that quasiparticle weight in the single-particle charge carrier spectral density denoted by Z^{-1} goes to zero logarithmically as the Fermi energy is approached. In this limit, there are no well-defined quasiparticle poles, and the entire spectral density consists of an incoherent background which is due to the interactions. It is the δ-function-like quasiparticle contribution (broadened by the interaction) which leads to a Drude-like contribution in the optical conductivity.[6,7] The incoherent background is responsible for the Holstein tails due, for example, to phonon-assisted absorption in the well-studied case of the electron-phonon interaction. The incoherent contribution to the optical conductivity gives additional information on correlation effects complementary to the Drude response. Both contributions are described microscopically by the electron self-energy $\Sigma(\omega)$ vs ω, which is the fundamental quantity about which we would like information from measurements on the optical conductivity $\sigma(\omega)$. For example, the real part (Σ_1) of Σ deals with mass renormalization of the quasiparticles and the imaginary part (Σ_2) is related to their lifetimes. As we have just described, Σ can also lead to an incoherent background.

One of the most striking manifestation of correlation effects in the high-T_c superconducting cuprates are the pseudogap features observed in their normal state. They are particularly prominent in underdoped systems, but are also known to be present at optimum doping.[2] The precise origin of the pseudogap is not yet known and this remains a controversial area. Nevertheless, the experimental situation is reasonably well characterized and has been reviewed by Timusk and Statt.[2]

The pseudogap has been identified as a distinctive and sometimes even abrupt change in the temperature variation of the nuclear spin lattice relaxation,[8] of the Knight shift,[9] of the dc resistivity,[10,11] and of the specific heat,[12–14] in the frequency dependence of the infrared conductivity[3,15] and the current voltage characteristics of a tunneling junction,[16] as well as in angular-resolved photoemission spectroscopy (ARPES).[17–19] This last experimental technique is particularly powerful and has revealed that the pseudogap is not constant around the Fermi surface. Rather it has a *d*-wave nature which is the same symmetry as is exhibited by the superconducting gap below T_c in the cuprates.

That the pseudogap has its origin in correlation effects is not in doubt. Rather, the issue is how it is to be simply, yet accurately, described.[20–26] Many theoretical suggestions have been made. One widely held view is based on the so-called preformed pair model in which it is envisioned that the Cooper pairs exist above T_c up to a higher pseudogap temperature T^*, but without phase coherence. The phase coherence between the pairs, which is essential for superconductivity, sets in only at lower temperature $T<T_c$.[23,24] In another model, different but related, finite-momentum pairs are believed to be responsible for the pseudogap features.[25] A very different recent proposal is the suggestion of Chakravarty *et al.*[26] of *D*-density-wave formation with attended orbital currents which double the crystallographic unit cell. There are also proposals encoded in the ideas of spin-charge separation[21,22] and the pioneering suggestion of Anderson.[20]

The true nature of the changes that are brought about in the energy-dependent electronic density of states (EDOS) $N(\epsilon)$ by the formation of the pseudogap remains unknown other than that the EDOS is depressed in some way. Consequently we will not address this specific case directly here although it is a motivating force for what we have done. Instead we will be concerned with a related but less specific

issue–namely, the general question of how changes in $N(\epsilon)$ around the Fermi energy will manifest themselves in corresponding changes in the frequency dependence of the optical conductivity $\sigma(\omega)$ vs ω. After all, from an experimental point of view, it is important to understand what qualitative signature is to be looked for which corresponds to microscopic changes in $N(\epsilon)$.

To remain as simple as possible, we will examine in this paper in some detail mainly a simple model for $N(\epsilon)$ which consists of a constant background N_b modified by two Lorentzian forms, both chosen to be symmetric about the Fermi energy. This assumption allows us to take advantage of the mathematical simplifications associated with the existence of particle-hole symmetry. In addition, one of the Lorentzian form is taken to add states to N_b, while the other subtracts states so that there is conservation of total number of states when $N(\epsilon)$ is integrated over energy, i.e., $\int_{-\infty}^{\infty}\Delta N(\epsilon)d\epsilon=0$, where $\Delta N(\epsilon)$ is the change in the EDOS. The Lorentzian form has the important simplifying property that an energy integral in the definition of the conductivity can be done analytically.

For simplicity we also limit ourselves to the case of elastic impurity scattering. This case has been extensively studied in the approximation that $N(\epsilon)$ is constant in the energy range about the Fermi energy which is significant for transport. For a constant N_b the quasiparticle scattering rate $1/\tau_{\rm qp}(\omega)\equiv-\Sigma_2(\omega)$ is constant, independent of energy ω. The conductivity takes on the well-known Drude form with constant transport scattering rate which gives the half-width of the Drude and is in fact equal to twice the quasiparticle scattering rate. When inelastic scattering is considered, the quasiparticle scattering rate can still be defined in terms of the self-energy $\Sigma_2(\omega)$, but now it acquires a temperature and frequency dependence.[6,7] In this case, the quasiparticle scattering time $\tau_{\rm qp}(\omega)$ is no longer equal to the optical scattering time $\tau_{\rm op}(\omega)$, which is formally defined in terms of $\sigma(\omega)=\sigma_1(\omega)+i\sigma_2(\omega)$ through the formula

$$\frac{1}{\tau_{\rm op}(\omega)}=\frac{\Omega_p^2}{4\pi}{\rm Re}\frac{1}{\sigma(\omega)}=\frac{\Omega_p^2}{4\pi}\frac{\sigma_1(\omega)}{\sigma_1^2(\omega)+\sigma_2^2(\omega)}, \tag{1}$$

where Ω_p is the plasma frequency which is related to the real part of the conductivity $\sigma_1(\omega)$ through the optical oscillator strength sum rule

$$\int_0^{\infty}d\omega\,\sigma_1(\omega)=\frac{\Omega_p^2}{8}. \tag{2}$$

In contrast to the constant EDOS case, when $N(\epsilon)$ varies with ϵ around the Fermi energy, $1/\tau_{\rm qp}$ and $1/\tau_{\rm op}$ are no longer constant just as in the inelastic case and are not equal. Each acquires a separate dependence on energy. The imaginary part of the electron self-energy $\Sigma_2(\omega)$ becomes proportional to the self-consistent quasiparticle density of states $\tilde{N}(\omega)$ of the impure system. Impurities broaden the pure crystal EDOS $N(\epsilon)$, leading to $\tilde{N}(\omega)$. The optical scattering time defined in Eq. (1) also acquires ω dependence and can be quite different from the quasiparticle scattering time,[6,7] which is measured in ARPES experiments. Thus, optical and ARPES data give complementary information on $\Sigma(\omega)$. What is measured in ARPES is the single-particle spectral density for a particular momentum $\mathbf{k}$ as a function of ω. It is denoted by $A(\mathbf{k},\omega)$ and is related to the self-energy $\Sigma(\omega)$, with $\mathbf{k}$ dependence suppressed, by

$$A(\mathbf{k},\omega)=-\frac{1}{\pi}\frac{\Sigma_2(\omega)}{[\omega-\epsilon_{\mathbf{k}}-\Sigma_1(\omega)]^2+\Sigma_2^2(\omega)}. \tag{3}$$

The interpretation of optical results is now no longer straightforward. As an example of the complications that arise we note that for the case (as we will assume in most of our calculations here) when $N(\epsilon)$ conserves states, the integral over energy of the ARPES rate will also remain unchanged. This is because $1/\tau_{\rm qp}(\omega)$ is proportional to $\tilde{N}(\omega)$ and $\int_{-\infty}^{\infty}\Delta\tilde{N}(\epsilon)d\epsilon=0$ is guaranteed when $\int_{-\infty}^{\infty}\Delta N(\epsilon)d\epsilon=0$. This sum rule, however, does not hold for $1/\tau_{\rm op}(\omega)$, as has been previously discussed[27,28] for the case of inelastic scattering processes and for the onset of superconductivity, with constant EDOS. Nor is the total optical oscillator strength defined in Eq. (2) constant. This arises because the integral over $\sigma_1(\omega)$ defining Ω_p depends on an average of the EDOS $N(\epsilon)$ around the Fermi energy over an energy scale defined by the impurity scattering and is not just dependent on $N(0)$ as it would be in the familiar constant EDOS case. There is also an attendant temperature dependence of Ω_p. As the temperature becomes comparable to the energy scale on which $N(\epsilon)$ varies significantly, the energy dependence in $N(\epsilon)$ is effectively smeared out and we recover a simple Drude form.

The energy-dependent EDOS enters the formula for the conductivity in two places. First, the total current is the sum of the partial currents contributed by each state $|\mathbf{k}\rangle$ in the electron system. When this sum is changed into an integral over energy a first factor of $N(\epsilon)$ enters. But there is a second factor of $N(\epsilon)$ that also comes in from the quasiparticle scattering rate. This rate is proportional to the matrix element of the impurity potential which is to be averaged over all final states in which the electron can scatter. We can call this a final-state effect. This second factor enters the ARPES rate which becomes proportional to the self-consistent $\tilde{N}(\omega)$. Clearly, ARPES and optical rates can no longer simply be proportional to each other. Both the initial- and final-state factors modify the optical scattering rate.

In our calculations, we find that the factor of $N(\epsilon)$ coming from the sum over partial currents from each electron has less of an effect on the energy dependence of $\sigma_1(\omega)$ than does the modification of the underlying ARPES rate due to final-state effects. For a model of $N(\epsilon)$ which has a depression in the EDOS at $\epsilon=\epsilon_F$, which is, of course, compensated for at higher energies so as to conserve the total number of states, the first factor of $N(\epsilon)$ decreases the dc conductivity more than at finite frequency so that the overall effect is to lead to an apparent broadening of the Drude-like form for $\sigma_1(\omega)$. On the other hand, the ARPES rate is effectively reduced at small ω by the final-state factor of $\tilde{N}(\epsilon)$. This sharpens the Drude-like line at small ω. Thus the two

effects have opposite tendencies, compete against each other, and partially cancel. In the specific cases considered, the modifications in $\sigma_1(\omega)$ brought about by the changes in the ARPES rate are more important.

In a final set of calculations we also consider the case of a step-function EDOS model. In a metal $N(\epsilon)$ is expected to be finite at the Fermi energy although it could be small as compared to its value away from the Fermi energy. With our step model we show that a small but finite value h of $N(\epsilon)$ for $|\epsilon|<$ some energy E_g about $\epsilon=0$ always leads to the existence of a Drude-like peak in the optical response, in sharp contrast to the case $h=0$ when a gap forms and the Drude peak is completely eliminated.

The paper is organized as follows. In Sec. II, we present a general theory of the optical conductivity in the case of impurity scattering. Section III is devoted to a discussion of the effect of the energy-dependent EDOS on optical conductivity, within a toy model for the EDOS involving two Lorentzian forms. This is followed by a parallel discussion, in Sec. IV, for another EDOS model, the step model, which allows us to contrast metalliclike and semiconductinglike behavior. Finally, Sec. V contains our conclusion. Some mathematics is shown in Appendixes A and B.

II. GENERAL THEORY FOR OPTICAL CONDUCTIVITY

In linear response theory, the real and imaginary parts of the optical conductivity can be expressed, under the assumption that vertex corrections are negligible, as[29]

$$\sigma_1(\omega)=\frac{\Omega_{p0}^2}{4\pi}\pi\int_{-\infty}^{\infty}d\epsilon\frac{N(\epsilon)}{N_b}\int_{-\infty}^{\infty}\frac{dx}{\omega}f(x)\times A(\epsilon,x)[A(\epsilon,x+\omega)-A(\epsilon,x-\omega)], \tag{4}$$

$$\sigma_2(\omega)=\frac{\Omega_{p0}^2}{4\pi}\int_{-\infty}^{\infty}d\epsilon\frac{N(\epsilon)}{N_b}\int_{-\infty}^{\infty}\frac{dx}{\omega}f(x)A(\epsilon,x)\times[G_1(\epsilon,x+\omega)+G_1(\epsilon,x-\omega)-2\,G_1(\epsilon,x)], \tag{5}$$

where $N(\epsilon)/N_b$ is the normalized EDOS with N_b the constant background EDOS, $f(x)$ the Fermi distribution function, $G_1(\epsilon,x)$ the real part of the quasiparticle Green function $G(\epsilon,x\pm i\delta)$, and Ω_{p0} the bare plasma frequency which, for an energy-dependent EDOS, will be shown below to be different from the real plasma frequency Ω_p defined in Eq. (2). $A(\epsilon,\omega)$ is the spectral density defined in Eq. (3). In the case of elastic scattering with no momentum dependence (no anisotropy), $G(\epsilon,x)$ can be written as

$$G(\epsilon,x\pm i\delta)=[x-\epsilon-\Sigma_1(x)\pm ig(x)]^{-1}, \tag{6}$$

where $g(x)=|\Sigma_2(x)|=\tau_{\rm qp}^{-1}(x)$ the quasiparticle scattering rate. $\Sigma_1(x)$ and $g(x)$ satisfy the Kramers-Kronig (KK) relation.

Equations (4) and (5) show how the two effects of the energy-dependent EDOS mentioned in the Introduction enter: one is the factor $N(\epsilon)$ coming from the sum over partial currents from each electron in the Fermi sea; the other arises from the electron spectral density factor $A(\mathbf{k},\omega)$, which contains a factor of the final states the particles are scattered into.

The real and imaginary parts of the conductivity, σ_1 and σ_2, respectively, obey the KK relation, which together with Eq. (2) leads to the useful relationship, $\lim_{\omega\to\infty}\sigma_2(\omega)=\Omega_p^2/4\pi\omega$. At zero T, Eq. (4) simplifies greatly and becomes

$$\sigma_1(\omega)=\frac{\Omega_{p0}^2}{4\pi}\pi\int_{-\infty}^{\infty}d\epsilon\frac{N(\epsilon)}{N_b}\int_{-\omega}^{0}\frac{dx}{\omega}A(\epsilon,x)\,A(\epsilon,x+\omega). \tag{7}$$

The dc conductivity immediately reads

$$\sigma(0)=\frac{\Omega_{p0}^2}{4\pi}\frac{1}{\pi}\int_{-\infty}^{\infty}d\epsilon\frac{N(\epsilon)}{N_b}\frac{g^2(0)}{[\epsilon^2+g^2(0)]^2}. \tag{8}$$

We assume that the impurity potential V is small and thus the impurity scattering can be treated perturbatively. Within the *self-consistent* Born approximation, the self-energy reads

$$\Sigma_{\rm sc}^{(\rm ret)}(\omega)=\Sigma_{1\rm sc}(\omega)-ig_{\rm sc}(\omega)=\gamma_0\int_{-\infty}^{\infty}d\epsilon\frac{N(\epsilon)}{N_b}G(\epsilon,\omega+i\delta), \tag{9}$$

where $\gamma_0=n_iV^2N_b$ with n_i the impurity density. The full self-consistent G appears on the right-hand side of Eq. (9), so this equation must be solved by successive iteration until convergence is achieved. Replacing G by $(\omega-\epsilon+i\delta)^{-1}$ on the right-hand side of Eq. (9) gives instead the *non-self-consistent* self-energy $\Sigma_{\rm nsc}^{(\rm ret)}(\omega)=\Sigma_{1\rm nsc}(\omega)-ig_{\rm nsc}(\omega)$.

In the case of a constant EDOS, $N(\epsilon)\equiv N_b$, $\Sigma_1\equiv 0$, $g(\omega)\equiv\pi\gamma_0=\Gamma/2$. Equations (4) and (5) thus result in the well-known Drude formula. $\sigma_1^{(\rm Drude)}(\omega)$ is a Lorentzian function of ω with the half-width Γ. We immediately find from Eq. (1) that $\tau_{\rm op}^{-1}(\omega)^{(\rm Drude)}\equiv 2g(\omega)=\Gamma$. In this simple case, the optical scattering rate is just equal to twice the quasiparticle scattering rate. Thus optical experiments access directly the microscopic information on the imaginary part of the self-energy. Further, the dc conductivity and the plasma frequency become $\sigma^{(\rm Drude)}(0)=\Omega_{p0}^2/(4\pi\Gamma)$, $\Omega_p^{(\rm Drude)}=\Omega_{p0}$. In Figs. 3 and 4 below, $\sigma_1^{(\rm Drude)}(\omega)$ and $\tau_{\rm op}^{-1}(\omega)^{(\rm Drude)}$ as functions of ω are shown as dot-dashed lines and serve as a reference when we discuss the effects on the optical conductivity of an energy dependence in the EDOS.

It is important at this point to emphasize that although, as we have stated, we have neglected corrections to the electromagnetic vertex, the bare vertex itself can introduce further complications in Eqs. (4) and (5). Besides the EDOS factor $N(\epsilon)$, there is also a factor of the square of the Fermi velocity which is the electromagnetic vertex in our work, and this factor can have energy dependence. As we will not evaluate $N(\epsilon)$ or for that matter the electron velocity $v(\epsilon)$ from first principles[30] but rather simply use a Lorentzian model, we can think that our model for the EDOS already contains the Fermi velocity and any dependence it may have on energy ϵ. There is one caution we should make, however. As shown in

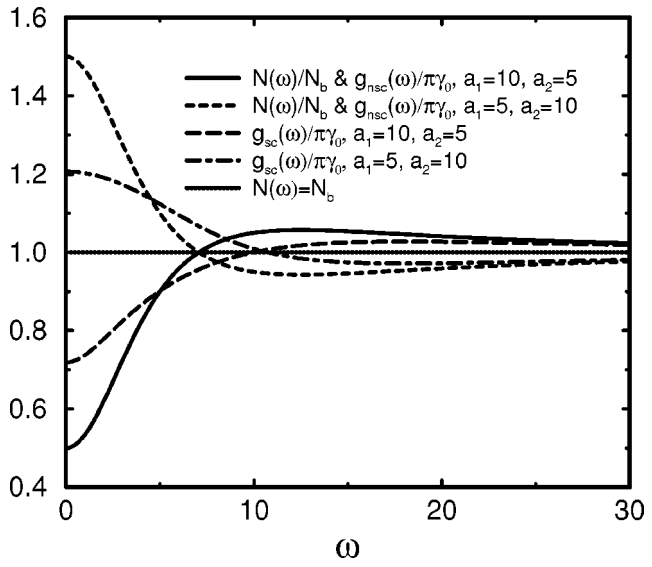

FIG. 1. Normalized EDOS and ARPES scattering rate as functions of frequency in the Lorentzian-EDOS model shown in Eq. (10). We used $s=5\pi$. All energies are in units of γ_0.

Eq. (9), in our discussion of the quasiparticle scattering rate, a second factor of the EDOS enters and this one is not multiplied by the electron velocity squared. This second factor will further get renormalized by the impurity scattering and so is replaced everywhere by the dressed EDOS $\tilde{N}(\omega)=-\int d\epsilon[N(\epsilon)/N_b]A(\epsilon,\omega)$. [Note that $g_{sc}(\omega)$ in Eq. (9) is directly proportional to the renormalized EDOS $\tilde{N}(\omega)$.] This should allow us to distinguish between the effects of these two factors of EDOS as we discuss below, and we will not emphasize this complication further but it should be kept in mind.

III. OPTICAL CONDUCTIVITY FOR EDOS WITH TWO LORENTZIAN FORMS

Now we are in the position to study the influence of the energy dependence of EDOS on the optical conductivity. In this section, we consider the following model for EDOS,

$$\frac{N(\epsilon)}{N_b}=1+\frac{s}{\pi}\left(\frac{a_1}{a_1^2+\epsilon^2}-\frac{a_2}{a_2^2+\epsilon^2}\right), \tag{10}$$

where $s>0$. The two Lorentzian forms of Eq. (10) guarantee conservation of the total states: $\int_{-\infty}^{\infty}\Delta N(\epsilon)d\epsilon=\int_{-\infty}^{\infty}[N(\epsilon)-N_b]d\epsilon=0$. For $a_1>a_2$, there is a hole—i.e., depletion of states—around the Fermi surface. This is shown as the solid line in Fig. 1. Whereas $a_1<a_2$ corresponds to a peak, namely, additional states at and around the Fermi surface, as shown by the dashed line in the same figure. The excess (missing) states are compensated for by a decrease (increase) in $N(\epsilon)$ at higher energies beyond $\epsilon=\sqrt{a_1a_2}\simeq 7$ in units of γ_0 for $a_1=5$, $a_2=10$ ($a_1=10$, $a_2=5$).

Equations (9) and (10) yield

$$\Sigma_{1sc}(\omega)=\gamma_0 s\left(\frac{\omega_0}{\omega_0^2+g_{a1}^2}-\frac{\omega_0}{\omega_0^2+g_{a2}^2}\right), \tag{11}$$

$$g_{sc}(\omega)=\pi\gamma_0+\gamma_0 s\left(\frac{g_{a1}}{\omega_0^2+g_{a1}^2}-\frac{g_{a2}}{\omega_0^2+g_{a2}^2}\right), \tag{12}$$

where $\omega_0=\omega-\Sigma_{1sc}(\omega)$, $g_{a1}=g_{sc}(\omega)+a_1$, and $g_{a2}=g_{sc}(\omega)+a_2$. Equations (11) and (12) can be easily solved numerically. Setting $\Sigma_{1sc}(\omega)=g_{sc}(\omega)=0$ on the right-hand side of Eqs. (11) and (12) we get the non-self-consistent self-energy. The solid line and the dashed line shown in Fig. 1 also represent $g_{nsc}/\pi\gamma_0$ vs ω.

There exists an extensive literature on the effect of energy dependence of the EDOS on the electron self energy and on other properties.[31–37] Some aspects of the superconducting state as well as normal state have been explored although much of the literature deals with a peak such as in a van Hove singularity model, while here we have emphasized a pseudogap. The imaginary parts g_{sc} obtained from Eqs. (11) and (12) for $a_1>a_2$ and for $a_2>a_1$ are shown in Fig. 1 as the long-dashed line and dot-dashed line, respectively. Comparing g_{nsc} and g_{sc} in Fig. 1, we see that self-consistency smoothes out the ARPES rate because it is broadened out by impurity scattering. In fact, this rate is simply proportional to the fully renormalized EDOS $\tilde{N}(\epsilon)$ defined by Eq. (12) with factor $\pi\gamma_0$ left out. Equation (12) has the same form as Eq. (10) with the broadening in the Lorentzian forms. In Fig. 1 we see that for the case of the hole (peak) at the Fermi surface $N(\epsilon)/N_b$ at $\epsilon=0$ is 0.5 (1.5) and the application of self-consistency changes these numbers to about 0.7 (1.2). The smearing due to the impurity scattering is considerable in the EDOS.

A. Constant ARPES rate $g(\omega)=\Gamma/2$ but energy-dependent $N(\epsilon)$

As we mentioned in the Introduction, there are two effects of EDOS on the optical conductivity: one is from summing over partial currents, which shows up as the explicit factor of $N(\epsilon)$ in Eqs. (4) and (5); the other is the final-state effect entering in the ARPES rate which shows up in Eq. (12). To see clearly the different roles these two effects play, we first switch off the effect of energy-dependent ARPES rate and replace it by a constant $g(\omega)=\Gamma/2$. Correspondingly, $\Sigma_1=0$.

We focus on the $T=0$ case, because it is simplest and allows us to produce partially analytic results. Eqs. (7) and (5) immediately yield

$$\sigma_1(\omega)=\frac{\Omega_{p0}^2}{4\pi}\frac{1}{\pi}\int_{-\infty}^{\infty}d\epsilon\frac{N(\epsilon)}{N_b}\mathcal{J}_{\Gamma/2}^{(re)}\left(\frac{\omega}{\Gamma/2},\frac{\epsilon}{\Gamma/2}\right), \tag{13}$$

$$\sigma_2(\omega)=\frac{\Omega_{p0}^2}{4\pi}\frac{1}{\pi}\int_{-\infty}^{\infty}d\epsilon\frac{N(\epsilon)}{N_b}\mathcal{J}_{\Gamma/2}^{(im)}\left(\frac{\omega}{\Gamma/2},\frac{\epsilon}{\Gamma/2}\right), \tag{14}$$

where

$$\mathcal{J}_{\gamma}^{(re)}(\tilde{\omega},e)=2t_{\gamma}(S_1+S_2/\tilde{\omega}), \tag{15}$$

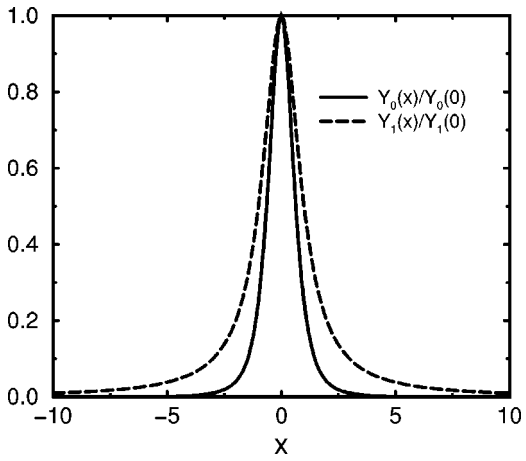

FIG. 2. Scaling functions $Y_0(x)=2/[\pi(x^2+1)^2]$ and $Y_1(x)=2/[\pi(x^2+1)]$.

$$\mathcal{J}_\gamma^{(\mathrm{im})}(\tilde{\omega},e)=t_\gamma[S_2-4S_1/\tilde{\omega}+1/(e^2+1)], \tag{16}$$

with $t_\gamma=1/[\gamma^2\tilde{\omega}(\tilde{\omega}^2+4)]$, $S_1=\arctan(\tilde{\omega}+e)$, and $S_2=\ln\{[(\tilde{\omega}+e)^2+1]/(e^2+1)\}$. The expressions for the dc conductivity and plasma frequency become particularly simple and very revealing. From Eqs. (8) and (2) we get

$$\sigma(0)=\frac{\Omega_{p0}^2}{4\pi}\frac{2}{\Gamma}\int_0^\infty dx\frac{N(x\Gamma/2)}{N_b}Y_0(x), \tag{17}$$

$$\frac{\Omega_p^2}{8}=\frac{\Omega_{p0}^2}{8}\int_0^\infty dx\frac{N(x\Gamma/2)}{N_b}Y_1(x), \tag{18}$$

where $Y_0(x)=2/[\pi(x^2+1)^2]$ and $Y_1(x)=2/[\pi(x^2+1)]$. We have plotted the two functions $Y_0(x)$ and $Y_1(x)$ in Fig. 2. Both peak at $x=0$, and decay rapidly on a scale of ϵ equal to a few times $\Gamma/2$. For small Γ, both $\sigma(0)$ and Ω_p depend strongly on the EDOS at and around the Fermi surface. If $N(\epsilon\simeq 0)<N_b$, which is the case for $a_1>a_2$, $\sigma(0)<\sigma^{(\mathrm{Drude})}(0)$ and $\Omega_p<\Omega_{p0}$ immediately follow. In the opposite case for $a_1<a_2$ in which $N(\epsilon\simeq 0)>N_b$, we get $\sigma(0)>\sigma^{(\mathrm{Drude})}(0)$ and $\Omega_p>\Omega_{p0}$. Besides, the peak in $Y_1(x)$ is broader than that in $Y_0(x)$, implying that the dc conductivity and the plasma frequency $\sigma(0)$ and Ω_p do not scale with each other for energy-dependent EDOS. The region in energy around the Fermi energy that is most important in determining $\sigma(0)$ and Ω_p^2 is given by Γ. If, as we have assumed so far, the scale for Γ is much less than the energy scale that controls important variations in the EDOS which in our case is (a_1,a_2) in the Lorentzian form, then it is mainly the value of $N(\epsilon)$ at $\epsilon=0$ which comes in. But when Γ is of the same order as (a_1,a_2), this is no longer the case and the details of the variations in $N(\epsilon)$ are importantly sampled. Finally when Γ is much greater than (a_1,a_2), it will be only the size of the background N_b that matters. This is the limit in which we regain the simple Drude model.

It is easy to find from Eqs. (14) and (18) that $\lim_{\omega\to\infty}\sigma_2(\omega)=\Omega_p^2/4\pi\omega$, indicating the KK relation is automatically obeyed as we expect. For a general value of ω, σ_1 and σ_2 in Eqs. (13) and (14) need to be obtained numerically. Inserting results of Eqs. (13), (14), and (18) into Eq. (1) allows us to obtain the optical scattering rate. Results will be discussed in Sec. III C.

B. Constant $N(\epsilon)$ but energy-dependent ARPES rate $g(\omega)$

If instead we switch off the energy-dependent EDOS by replacing it with $N(\epsilon)=N_b$, but turn on the energy-dependent ARPES rate $g(\omega)$ alone, we are able to see the final-state effect on σ, coming from the ARPES rate alone. Since in the present work the self-energy is momentum independent, it is convenient to first integrate over ϵ in Eqs. (7) and (5) at $T=0$. After some algebra we obtain

$$\sigma_1^{(\mathrm{cons})}(\omega)=\frac{\Omega_{p0}^2}{4\pi}\frac{1}{\pi}\lim_{D\to\infty}\int_{-\omega}^0\frac{dx}{\omega}\frac{1}{g(x)}\mathcal{F}^{(\mathrm{re})}(\tilde{D},g_+,x_0,x_+)$$
$$=\frac{\Omega_{p0}^2}{4\pi}\int_{-\omega}^0\frac{dx}{\omega}\frac{1}{g(x)}\frac{g_++1}{(g_++1)^2+(x_0-x_+)^2}, \tag{19}$$

$$\sigma_2^{(\mathrm{cons})}(\omega)=\frac{\Omega_{p0}^2}{4\pi}\frac{1}{\pi}\lim_{D\to\infty}\int_{-\infty}^0\frac{dx}{\omega}\frac{1}{g(x)}$$
$$\times\left[\sum_{i=\pm}\mathcal{F}^{(\mathrm{im})}(\tilde{D},g_i,x_0,x_i)-\mathcal{F}_0^{(\mathrm{im})}(\tilde{D},x_0)\right]$$
$$=\frac{\Omega_{p0}^2}{4\pi}\int_{-\omega}^0\frac{dx}{\omega}\frac{1}{g(x)}\frac{x_+-x_0}{(g_++1)^2+(x_0-x_+)^2}, \tag{20}$$

where $\tilde{D}=D/g(x)$, $x_0=[x-\Sigma_1(x)]/g(x)$, $g_\pm=g(x\pm\omega)/g(x)$, $x_\pm=[x\pm\omega-\Sigma_1(x\pm\omega)]/g(x)$, and $\mathcal{F}^{(\mathrm{re})}$, $\mathcal{F}^{(\mathrm{im})}$, and $\mathcal{F}_0^{(\mathrm{im})}$ defined in Eqs. (A1)–(A3) in Appendix A.

C. Energy-dependent $N(\epsilon)$ and ARPES rate

If we want to include both the direct factor of $N(\epsilon)$ in Eqs. (4) and (5) and the energy-dependent ARPES rate so as to study the competition between the initial-state effect and the final-state effect, we need to insert $N(\epsilon)$ into Eq. (10) and $g_{\mathrm{sc}}(\omega)$ into Eq. (12) or $g_{\mathrm{nsc}}(\omega)$ into Eqs. (7) and (1) to find $\sigma_1(\omega)$ and $\tau_{\mathrm{op}}^{-1}(\omega)$. The Lorentzian forms used for $N(\epsilon)$ allow us to do the integral over ϵ analytically. The expressions for $\sigma_1(\omega)$ and $\sigma_2(\omega)$ are given in Appendix B.

Our first numerical results are presented in Fig. 3, which has two complementary frames (a) and (b). In all curves $a_1=10$, $a_2=5$ with $s=5\pi$, in units of γ_0. This corresponds to a depression in the EDOS [see Eq. (10)] over its background value, as drawn in Fig. 1, solid curve, with $N(0)$ reduced by a factor of 2 compared to the background value. Although electronic states are preserved, this does not mean that the corresponding optical oscillator strength is, as we will see. In Fig. 3(a) we show five curves. All give the real part of the optical conductivity $\sigma_1(\omega)$ in units of $\Omega_{p0}^2/4\pi$ as a function of energy ω in units of γ_0. The first one (dot-dashed line) is for reference and is the usual Drude form. In this case, the width of the Drude is simply $2\pi\gamma_0\equiv\Gamma$ and the oscillator sum rule gives $\Omega_{p0}^2/8$. This no longer holds when the energy

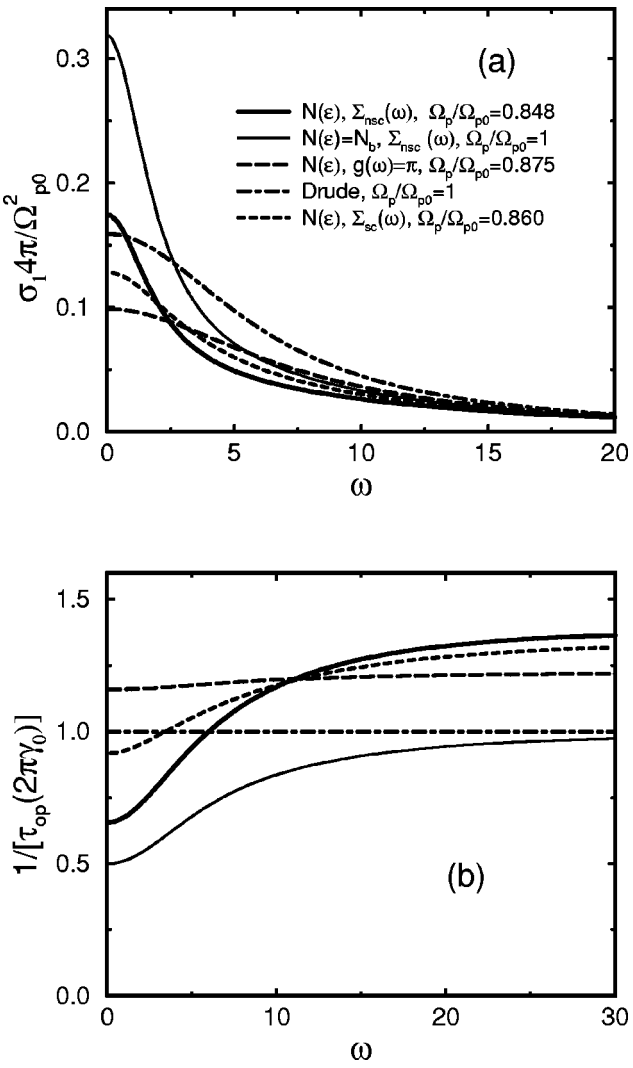

FIG. 3. (a) Real part of optical conductivity and (b) optical scattering rate as functions of frequency in the Lorentzian-EDOS model shown in Eq. (10) with $a_1=10$, $a_2=5$, and $s=5\pi$. We used $\gamma_0=1$. Labels of curves in (b) mean the same as in (a).

dependence is included in the EDOS. This leads to several modifications and we will take these in steps of added complications. The simplest modification is that an overall EDOS factor enters the sum over partial currents involving each participating electron. Including only this factor with a constant approximation for the scattering rate $g(\omega)=\pi$ in units of γ_0 gives the long-dashed curve. The factor of 2 reduction in $N(\epsilon)$ at $\epsilon=0$ translates into a substantial reduction in $\sigma_1(\omega)$ at $\omega=0$ although by a factor substantially less than 2. While the line shape is no longer perfectly Drude, its width at half maximum has increased over the Drude case $\Gamma=2\pi\gamma_0$ and could lead one to conclude that the optical scattering rate has increased. It is already clear from this remark that the optical and quasiparticle scattering rates are no longer the same. In fact, this is shown explicitly in Fig. 3(b). The dot-dashed curve is constant but the long-dashed curve now exhibits a slight energy dependence and is everywhere larger than twice the quasiparticle rate. Another important modification brought about by the introduction of an energy dependence in $N(\epsilon)$ is that the optical sum rule defined in Eq. (2) has the plasma frequency reduced from Ω_{p0} to $\Omega_p=0.875\,\Omega_{p0}$. Note that this occurs although no states are lost in $N(\epsilon)$. On the other hand, when the initial-state EDOS factor is taken to be independent of energy (constant N_b) there is no change in plasma frequency even if the quasiparticle scattering rate is energy dependent as shown in the solid thin curve which was computed for constant $N(\epsilon)=N_b$, but with $\Sigma_{\rm nsc}$ obtained in a non-self-consistent theory for the quasiparticle scattering rate. This modulates the scattering rate with precisely the same EDOS factor $N(\epsilon)$ that we used for the initial-state sum in the long-dashed curve. We see that in a real sense this factor has the opposite effect on the shape of the conductivity $\sigma_1(\omega)$ vs ω in that it increases its value at $\omega=0$, beyond what it is in the pure Drude case, and also effectively sharpens up the curve. This can be seen more quantitatively in Fig. 3(b) where the solid thin curve for the optical scattering rate falls everywhere below the dash-dotted curve of the Drude theory and also even further below the long-dashed curve. Combining these two effects brings us back closer to our original Drude than including each separately, at low frequencies where the effects are biggest. This expectation is born out in the solid curve which includes initial state $N(\epsilon)$ factor and non-self-consistent quasiparticle scattering rate $g_{\rm nsc}(\omega)$. Note that the plasma frequency $(\Omega_p/\Omega_{p0}=0.848)$ is not changed much from its value of 0.875 in the long-dashed curve, which shows that the plasma frequency is mainly sensitive to the initial $N(\epsilon)$ and is less sensitive to the details of the quasiparticle scattering rate. The corresponding optical scattering rate is shown as the solid curve in Fig. 3(b). This curve contrasts greatly with the previous two curves: long-dashed and solid thin. In both these curves there is no compensation in the scattering rate as compared to the Drude case in the sense that the long-dashed curve is always above and the solid thin curve always below. By contrast, the solid curve is below at small ω and above at larger ω. While there is some cancellation, no sum rule applies to the area under $1/\tau_{\rm op}(\omega)$ when it is integrated over ω. This represents a real difference between quasiparticle scattering rate and optical scattering rate since for the ARPES rate a sum rule does apply which is directly connected to the sum rule on $N(\epsilon)$. Thus, while optics can give microscopic information on scattering rates, it is not easy to relate the information so obtained with the characteristics of the self-energy which is, in the end, the fundamental quantity and is the quantity we would like to measure directly.

One final element of importance has been neglected so far. To get the effective scattering rate in a system with energy-dependent EDOS with impurities, it is necessary to solve the self-energy equation (9) self-consistently through repeated iteration of Eqs. (11) and (12). Impurities will smear out a valley in $N(\epsilon)$ and change it to its self-consistent value $\tilde{N}(\epsilon)$, which is what finally enters in the impurity scattering. When this is done we obtain a final curve for $\sigma_1(\omega)$ vs ω, the dashed curve of Fig. 3(a) and for the optical scattering rate in Fig. 3(b). As we would have expected, the self-consistency smoothes out the curves but this does not intro-

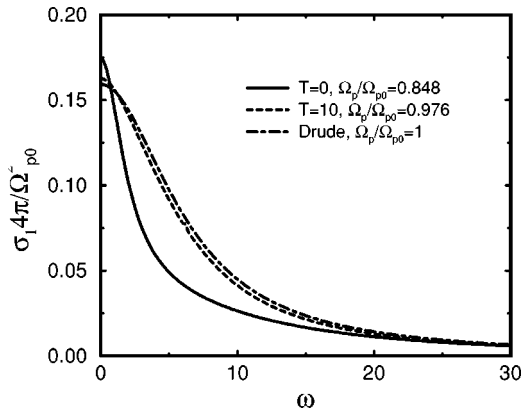

FIG. 4. Real part of the optical conductivity at different temperatures in the Lorentzian-EDOS model shown in Eq. (10). We used the same a_1, a_2, s, and γ_0 as in Fig. 3.

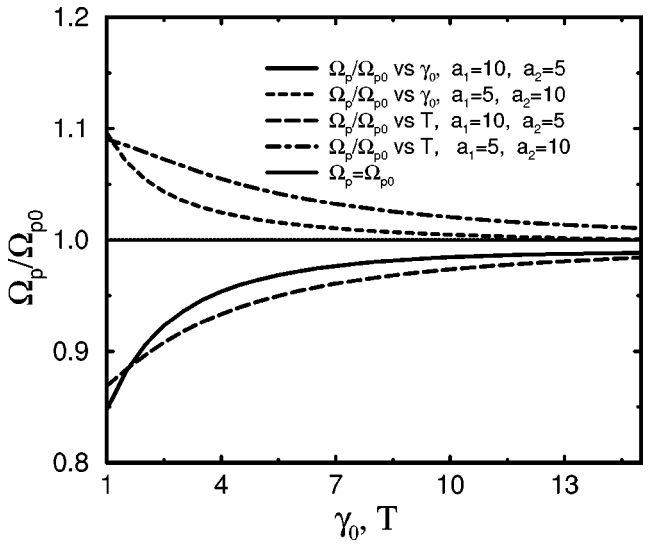

FIG. 5. Plasma frequency as a function of the impurity potential γ_0 and temperature T. We used $s=5\pi$.

duce any new physics. The value of the plasma frequency is also not changed much over its non-self-consistent value.

We bring up once more the complication that arises from the electromagnetic vertex which introduces a product of two electron velocity $v(\epsilon)^2$ in the formula for the conductivity which effectively introduces a further energy dependence in the factor of $N(\epsilon)$ appearing directly in Eqs. (4) and (5). This factor is not present in either the non-self-consistent self-energy or the self-consistent one shown in Eq. (9). This means that the dashed curve of Fig. 3(a) could be further modified through the introduction of a $v(\epsilon)^2$ factor in our model $N(\epsilon)$. If we look at band structure calculations, we note that the product of $N(\epsilon)v(\epsilon)^2$ is often less dependent on energy than is $N(\epsilon)$.[30,38] This means that in this case, the final results for the conductivity might move some way towards the results of a self-consistent theory for the self-energy with constant $N(\epsilon)$ as the explicit factor of EDOS in Eqs. (4) and (5)—i.e., those shown in Fig. 3(a) as the dotted line. The self-consistent case would be smoothed out a little more as compared with this curve.

We have also made calculations for a peak in the EDOS at the Fermi energy and found no new physics. The effects are in a real sense the opposite to those found for a depression.

Another consequence of the energy dependence in $N(\epsilon)$ is that the conductivity will change with temperatures, an effect which does not arise in the ordinary Drude case. This is illustrated in Fig. 4 where we show the real part of the conductivity $\sigma_1(\omega)$ vs ω for three cases. The solid curve repeats our previous results for the case of a gap at the Fermi energy and non-self-consistent ARPES rate, shown as the solid line in Fig. 3(a). The dot-dashed curve is the ordinary Drude for comparison. The dashed curve shows how the solid curve evolves with increasing temperature. It represents results of $\sigma_1(\omega)$ vs ω with non-self-consistent self-energy for temperature $T=10$ in units of γ_0 which is related to the quasiparticle scattering rate. It is clear that the evolution is towards restoring the curve to its simple Drude value as can be expected when temperature or impurity effects are sufficiently strong that they wash out the energy dependence in $N(\epsilon)$. Note that for the case considered here, the energy scale for the structure in $N(\epsilon)$ is 10 in our units and this scale is of the same order as the temperature. Similar smearing effects are expected when impurity scattering is increased sufficiently that the impurity scattering rate becomes comparable to the energy scale of the structure in $N(\epsilon)$. In this case we do not show a curve analogous to Fig. 4, but instead we show the change in the optical oscillator strength under the curve—i.e., the plasma frequency. Before presenting these results we point out that in Fig. 4 at $T=0$ the plasma frequency $\Omega_p/\Omega_{p0}=0.848$, while at $T=10$ it has moved up to 0.976 close to the simple Drude case, so that effects of energy dependence in $N(\epsilon)$ are pretty well washed out in Ω_p as they are in the full $\sigma_1(\omega)$ vs ω curve. In Fig. 5 we present equivalent results for the impurity scattering and compare with temperature. The dashed and dot-dashed lines are for a peak in $N(\epsilon)$ and the solid and long-dashed lines for a valley at the Fermi energy. We see that temperature and impurity have very similar effects on the plasma frequency and that when the scale on the horizontal axis is of the order of the scale defining the structure in $N(\epsilon)$, we recover in both cases the Drude plasma frequency as we expected.

IV. OPTICAL CONDUCTIVITY IN "STEP MODEL"

Another EDOS model which allows us to get simple analytical results and also helps in developing insight into the effect of $N(\epsilon)$ on $\sigma(\omega)$ is the so-called step model,

$$\frac{N(\epsilon)}{N_b}=\begin{cases} h, & |\epsilon|<E_g, \\ 1, & |\epsilon|>E_g. \end{cases} \tag{21}$$

The self-consistent self-energy from Eq. (9) is determined from the following equations:

$$\Sigma_{1\mathrm{sc}}(\omega)=(1-h)\frac{\gamma_0}{2}\ln\left[\frac{(\omega_0-E_g)^2+g_{sc}^2(\omega)}{(\omega_0+E_g)^2+g_{sc}^2(\omega)}\right], \quad (22)$$

$$g_{\mathrm{sc}}(\omega)=\gamma_0\left\{\pi-(1-h)\left[\arctan\left(\frac{\omega_0+E_g}{g_{\mathrm{sc}}(\omega)}\right)-\arctan\left(\frac{\omega_0-E_g}{g_{\mathrm{sc}}(\omega)}\right)\right]\right\}, \quad (23)$$

where $\omega_0=\omega-\Sigma_{1\mathrm{sc}}(\omega)$. While the non-self-consistent self-energy is obtained by making $\Sigma_{1\mathrm{sc}}(\omega)=g_{\mathrm{sc}}(\omega)=0$ on the right-hand side of Eqs. (22) and (23).

Inserting Eq. (21) into Eq. (7), we find that

$$\sigma_1(\omega)=\frac{\Omega_{p0}^2}{4\pi}\frac{1}{\pi}\int_{-\omega}^{0}\frac{dx}{\omega}\left\{\frac{1}{g(x)}\frac{\pi(\tilde{g}+1)}{(\tilde{g}+1)^2+(x_0-\tilde{x})^2}-(1-h)\mathcal{F}^{(\mathrm{re})}(\tilde{E}_g,\tilde{g},x_0,\tilde{x})\right\}, \quad (24)$$

where $\mathcal{F}^{(\mathrm{re})}$ is found in Appendix A, $\tilde{g}=g(x+\omega)/g(x)$, $x_0=[x-\Sigma_1(x)]/g(x)$, $\tilde{x}=[x+\omega-\Sigma_1(x+\omega)]/g(x)$, and $\tilde{E}_g=E_g/g(x)$.

In Fig. 6 we show the numerical results that we have obtained in the step model. Figure 6(a) gives the quasiparticle scattering rate $g(\omega)$ vs ω for four different cases. The dot-dashed line is the non-self-consistent result for $g(\omega)$ in the semiconductinglike model—i.e., $h=0$. We see that $g(\omega)$ is exactly zero until $\omega=10$ and jumps to π for $\omega>10$. This curve is for comparison with $g_{\mathrm{sc}}(\omega)$ in Eq. (23). The numerical results are the long-dashed curve. We see a sharp scattering edge at $\Omega_0\simeq 6.1$ below which the scattering rate is zero, so that now the sharp onset has moved to lower energy, as compared to the non-self-consistent case. Note that $g(\omega)$ is proportional to $\tilde{N}(\omega)$ and this shows smearing of the step function edge that existed in the non-self-consistent case. The impurity scattering also accounts for the reduction in scattering above $\omega=10$. In fact, there is a sum rule on $\tilde{N}(\omega)$ so that the area under each curve, self-consistent and non-self-consistent, remains unchanged. So the increase in fully renormalized EDOS below $\omega=10$ is fully compensated for at larger ω. This also holds for the second set of two curves. In this case $h=0.1$ instead of being zero. The dashed curve gives the non-self-consistent results while the solid curve is for the self-consistent case. In this case, there is always a finite EDOS at all frequencies, but it still rises sharply at $\omega=10$ in the non-self-consistent case and at $\omega\simeq 6.1$ in the self-consistent calculations. However, as compared with the $h=0$ case, the rise is less drastic. There is some rounding of the edge.

The corresponding results for $\sigma_1(\omega)$ vs ω are shown in Fig. 6(b). We see, as we expected, that for the pure semiconductorlike model, there is no optical absorption until $\omega=2E_g=20$ in the non-self-consistent case (dot-dashed curve). This also holds for the self-consistent case (long-dashed curve), but now the edge has moved to $\omega=2\Omega_0\simeq 12.2$. In the other two curves the finite value of $h=0.03$ at small ω guarantees that the response in this region is metallic like and we see a sharp Drude-like peak centered around $\omega=0$. At higher energy the semiconductinglike behavior of the two previous curves remains although the main rise in the conductivity has been shifted to lower ω as compared with $\omega=20$ and 12.2, respectively, for non-self-consistent and self-consistent case with $h=0$. Between the Drude response at small ω and semiconductinglike response at high ω the curve gets filled in and shows sharp structures corresponding to the sharp step assumed to exist in the initial EDOS $N(\epsilon)$.

We next contrast more sharply the two qualitatively different limits discussed above using an analytical method to get simple although limited results.

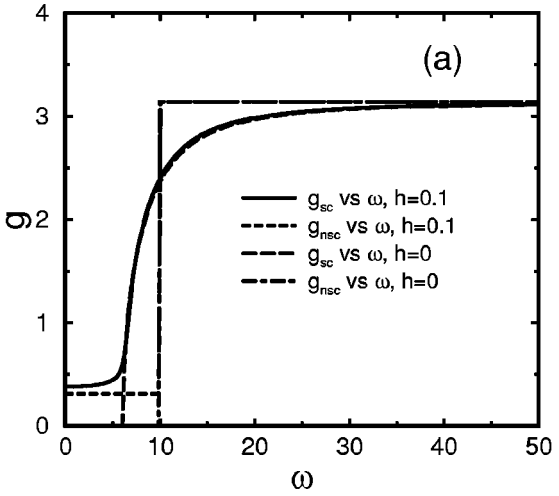

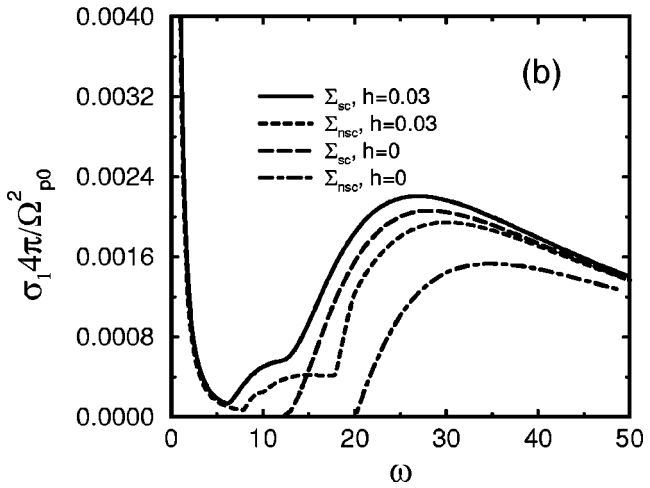

FIG. 6. (a) ARPES rate and (b) real part of the optical conductivity, as functions of frequency in the step model shown in Eq. (21). We used $E_g=10$ and $\gamma_0=1$.

A. $h=0$: Semiconductinglike behavior

In this case, $g(\omega)=0$ for $\omega<\Omega_0$. (Note that for the non-self-consistent ARPES rate, $\Omega_0=E_g$, and for the self-consistent ARPES rate, $\Omega_0<E_g$.)

Now we look at $\sigma_1(\omega)$ in Eq. (7). Noting that $-\omega<x<0$, we obtain the following.

(i) For $0<\omega<\Omega_0$, both $A(\epsilon,x)$ and $A(\epsilon,x+\omega)$ are zero, leading to $\sigma_1(\omega)=0$.

(ii) For $\Omega_0<\omega<2\Omega_0$, $A(x+\omega)=0$ for $-\omega<x<-\Omega_0$, while $A(x)=0$ for $-\Omega_0<x<0$. Therefore, $\sigma_1(\omega)=0$.

To conclude, $\sigma_1(\omega)=0$ for $\omega<2\Omega_0$.

B. $h=0^+$: Metalliclike behavior

In this case, we expect to see the Drude peak at small ω. This can be nicely shown in the dc conductivity. By substituting Eq. (21) into Eq. (8) we obtain

$$\sigma(0)=\frac{\Omega_{p0}^2}{4\pi}\frac{1}{\pi}\frac{1}{g(0)}\left\{(h-1)\left[\frac{E_g g(0)}{E_g^2+g^2(0)}+\arctan\left(\frac{E_g}{g(0)}\right)\right]+\frac{\pi}{2}\right\}. \tag{25}$$

It is clear that for $h=1$, Eq. (25) recovers the Drude result $\sigma^{(\mathrm{Drude})}(0)=(\Omega_{p0}^2/4\pi)/2g(0)$. In the limit of $h\to 0^+$, we get from Eq. (25) that

$$\sigma^{(h=0^+)}(0)\simeq\frac{\Omega_{p0}^2}{4\pi}\frac{h}{2g(0)}. \tag{26}$$

For the non-self-consistent case, $g_{\mathrm{nsc}}(0)=\pi\gamma_0 h$, thus

$$\sigma_{\mathrm{nsc}}^{(h=0^+)}(0)\simeq\frac{\Omega_{p0}^2}{4\pi}\frac{1}{2\pi\gamma_0}=\sigma^{(\mathrm{Drude})}(0). \tag{27}$$

For the self-consistent case, however, Eq. (23) produces, in linear order of h, $g_{\mathrm{sc}}(0)\simeq\pi\gamma_0 h/(1-2\gamma_0/E_g)$ (for $2\gamma_0<E_g$), leading to

$$\sigma_{\mathrm{sc}}^{(h=0^+)}(0)\simeq\frac{\Omega_{p0}^2}{4\pi}\frac{1}{2\pi\gamma_0}\left(1-\frac{2\gamma_0}{E_g}\right), \tag{28}$$

which is different from the corresponding Drude value.

We can also compare the above results obtained in the EDOS-step model for a finite h value with those obtained in the EDOS model with one Lorentzian form, $N(\epsilon)/N_b=1-(s/\pi)a_2/(a_2^2+\epsilon^2)$. We find that in the Lorentzian-form model, $\sigma_1(\omega)$ shows a sharp Drude-like peak at low frequencies and semiconductinglike rise at around $\omega\sim a_2$, which are similar to what is shown in the solid curve in Fig. 6. However, since both the EDOS and ARPES rates are smooth in this model, the conductivity curve is always smoothly evolving as a function of frequency, and the semiconductinglike rise can never be as sharp as in the step model.

V. CONCLUSION

We have studied the effect the energy dependence in the EDOS around the Fermi energy has on the frequency-dependent conductivity and the derived optical scattering rate. The conductivity is modified in two important ways. One comes from the energy-dependent EDOS factor which enters when a sum is to be carried out over all electrons that contribute to the current. We referred to this as the initial state factor. The second factor comes from modification of the quasiparticle scattering rate which is no longer constant and in fact becomes proportional to the self-consistent EDOS $\tilde{N}(\epsilon)$. This quantity differs from $N(\epsilon)$ in that it accounts for the smearing of the EDOS brought about by the impurities. It is to be computed from the self-consistent self-energy equations. Both factors have a profound effect on the conductivity, but their individual contribution cannot easily be separated. For a depression in $N(\epsilon)$ at the Fermi energy, the first factor reduces the real part of the conductivity at and around $\omega=0$ (dc conductivity), effectively making the resulting optical scattering rate appear larger than its value in the pure Drude model; i.e., the width of the curve at half maximum is increased. On the other hand, the second factor acts in the opposite manner. Since the quasiparticle scattering rate becomes proportional to $\tilde{N}(\omega)$, this quantity now acquires a frequency dependence which, in the model under consideration, reduces the scattering rate at and around $\omega=0$, because $\tilde{N}(\omega)$ is less than the constant background value there. This has the effect of increasing the height of the Drude at small ω and making it narrower as compared to the constant case. The net result of both effects in the self-consistent case is to produce a curve for $\sigma_1(\omega)$ vs ω which is reduced below the pure Drude at small ω. The corresponding optical scattering rate is depressed at small ω below its constant Drude value and then becomes larger at higher ω. This mimics the variation in the quasiparticle scattering rate which is proportional to $\tilde{N}(\omega)$, but there are important differences. In particular, while a sum rule applies to the ARPES scattering rate which reflects quite directly the sum rule on the EDOS, the optical scattering rate displays no such property. It is clear then that when there is important energy dependence in the EDOS at the Fermi energy, optical and quasiparticle scattering rates are not as simply related as in the Drude model. This complicates the process of extracting microscopic information from optical scattering rate data. What one ultimately wants is detail information on the self-energy.

There are several other complications that arise that need to be commented upon. The plasma frequency which gives the optical oscillator strength—i.e., the area under the real part of the conductivity—becomes dependent on temperature and on impurity concentration. It shows that the plasma frequency depends on a range of states around the Fermi energy with the width given by the impurity scattering rate. It is not just its value at the Fermi surface which matters. As the impurity rate is changed, the range of important values of $N(\epsilon)$ is also changed and so is Ω_p. In the models considered this can be a significant effect. Temperature can also smear out the region in energy around the Fermi surface and so also

impact on the value of Ω_p. As temperature is increased, we find that the EDOS effects become gradually less important and the entire curve for $\sigma_1(\omega)$ vs ω moves towards the Drude form with constant background only in $N(\epsilon)$. Another result of interest is that the region in energy most important in determining the plasma frequency is different from that determining the dc conductivity, so that these two quantities will not respond in the same way with a change in impurity content.

Finally we have considered a step-function model for $N(\epsilon)$ around the Fermi surface with $N(\epsilon)=hN_b$ for $0<\epsilon<E_g$, and $N(\epsilon)=N_b$ for $\epsilon>E_g$, where E_g is a gap energy. For $h=0$, this is a semiconductinglike model which leads directly to zero conductivity in the range $0\leqslant\omega\leqslant 2\Omega_0$ ($\Omega_0=E_g$ for the non-self-consistent ARPES rate and $\Omega_0<E_g$ for the self-consistent ARPES rate). We find that for finite h, however small it may be, the situation is radically different and an intrinsically metallic behavior is always obtained. At small ω, there is a very narrow Drude-like peak followed by a depression, and at higher energies $\omega\geqslant\Omega_0$ a semiconductinglike behavior is again observed. The value of the dc conductivity is unchanged from its value with $N(\epsilon)=N_b$ everywhere provided $h\ll 1$. Here we have described only the case when the self-energy is treated in a first iteration. We find, however, that the situation shows no qualitative change when a self-consistent theory is considered except for the important difference that the gap Ω_0 is reduced by the interactions and the dc conductivity has a correction linear in γ_0/E_g.

The theoretical calculations presented in this paper apply in principle to materials in which the EDOS has strong energy dependence around the Fermi surface. The experiments need to be done at relatively low temperatures where the electrons are dominantly scattered by impurities and the systems must remain in the normal state. Many conventional heavy fermion materials have energy-dependent EDOS and remain metallic down to very low temperatures and so may serve as potential candidates to show some features of optical conductivity within our predictions. In this case, our simple theoretical results caution against any interpretation based on a Drude model. The underdoped high-T_c cuprates exhibit a pseudogap of size 300 K or so. This pseudogap has its origin in many-body effects as we mentioned in the Introduction. Nevertheless, inasmuch as the effective EDOS around the Fermi surface is depressed, our results should give some qualitative guidance about the physical consequences of such a EDOS depression. It is clear from our simple work that this pseudogap cannot be treated in the usual formalism which assumes a constant effective EDOS. Of course, in the cuprates a superconducting transition occurs, but T_c can be low, of order 20 K. In this intermediate temperature regime, however, the inelastic scattering due to electronic interactions may already be significant, which complicates the comparison. Disordering in the CuO_2 planes, such as replacing copper sites by nickel, in the underdoped high-T_c cuprates, will efficiently enhance the elastic scattering, so that it becomes dominant. Alternatively, a magnetic field can be used to quench the superconductivity, enabling measurements at much lower temperatures.

ACKNOWLEDGMENTS

We thank E. J. Nicol for helpful discussions. This work is partially supported by the Natural Science and Engineering Research Council of Canada and by the Canadian Institute for Advanced Research.

APPENDIX A: EXPRESSIONS FOR $\mathcal{F}^{(\mathrm{re})}$, $\mathcal{F}^{(\mathrm{im})}$, AND $\mathcal{F}_0^{(\mathrm{im})}$ IN EQS. (19) AND (20)

As mentioned in Sec. III B, in the case of a constant $N(\epsilon)=N_b$ and energy-dependent ARPES rate, we can first integrate over ϵ. The resulting optical conductivity at $T=0$ is shown in Eqs. (19) and (20), where

$$\mathcal{F}^{(\mathrm{re})}(\tilde{D},g,x_0,x)=d_0[g(y^2+g^2-1)f_1+(y^2-g^2+1)f_2-gyf_3], \quad \text{(A1)}$$

$$\mathcal{F}^{(\mathrm{im})}(\tilde{D},g,x_0,x)=\frac{d_0}{2}[-2y(y^2+g^2+1)f_1+4gyf_2+(1-g^2+y^2)f_3], \quad \text{(A2)}$$

$$\mathcal{F}_0^{(\mathrm{im})}(\tilde{D},x_0)=4x_0\tilde{D}[(x_0-\tilde{D})^2+1]^{-1}\times[(x_0+\tilde{D})^2+1]^{-1}, \quad \text{(A3)}$$

with $d_0=[(g+1)^2+y^2]^{-1}[(g-1)^2+y^2]^{-1}$, $y=x_0-x$, $f_1=\arctan(\tilde{D}+x_0)+\arctan(\tilde{D}-x_0)$, $f_2=\arctan[(\tilde{D}+x)/g]+\arctan[(\tilde{D}-x)/g]$, and $f_3=\ln\{[(\tilde{D}-x_0)^2+1]/[(\tilde{D}+x_0)^2+1]\}+\ln\{[(\tilde{D}+x)^2+g^2]/[(\tilde{D}-x)^2+g^2]\}$.

APPENDIX B: OPTICAL CONDUCTIVITY FOR THE ENERGY-DEPENDENT ARPES RATE IN THE LORENTZIAN DOS MODEL

For the EDOS model with Lorentzian forms shown in Eq. (10) and energy-dependent ARPES rate, we can first integrate ϵ to simplify the numerical work. The resulting conductivity reads

$$\sigma_1(\omega)=\sigma_1^{(\mathrm{cons})}(\omega)+\delta\sigma_1(\omega,a_1)-\delta\sigma_1(\omega,a_2), \quad \text{(B1)}$$

$$\sigma_2(\omega)=\sigma_2^{(\mathrm{cons})}(\omega)+\delta\sigma_2(\omega,a_1)-\delta\sigma_2(\omega,a_2), \quad \text{(B2)}$$

where $\sigma_1^{(\mathrm{cons})}$ and $\sigma_2^{(\mathrm{cons})}$ are shown in Eqs. (19) and (20), and

$$\delta\sigma_1(\omega,a)=\frac{\Omega_{p0}^2}{4\pi}\frac{s}{2\pi}\int_{-\omega}^{0}\frac{dx}{\omega}\left[\frac{x_0x_1+g_{a+}g_{1a-}}{(x_0^2+g_{a+}^2)(x_1^2+g_{1a-}^2)}+\frac{x_0x_2-g_{a+}g_{2a+}}{(x_0^2+g_{a+}^2)(x_2^2+g_{2a+}^2)}\right]$$
$$+\frac{\Omega_{p0}^2}{4\pi}\frac{sa}{\pi}\int_{-\omega}^{0}\frac{dx}{\omega}\frac{2(x_1-x_0)x_1g_1+(g_0+g_1)(a^2+x_1^2-g_1^2)}{[(x_1-x_0)^2+(g_0+g_1)^2][(a^2+x_1^2-g_1^2)^2+4x_1^2g_1^2]},\tag{B3}$$

$$\delta\sigma_2(\omega,a)=\frac{\Omega_{p0}^2}{4\pi}\frac{s}{2\pi}\int_{-\infty}^{0}\frac{dx}{\omega}\left[\frac{x_2g_{a-}-x_0g_{2a+}}{(x_0^2+g_{a-}^2)(x_2^2+g_{2a+}^2)}+\frac{x_1g_{a+}-x_0g_{1a-}}{(x_0^2+g_{a+}^2)(x_1^2+g_{1a-}^2)}+\frac{x_0g_{1a+}+x_1g_{a+}}{(x_0^2+g_{a+}^2)(x_1^2+g_{1a+}^2)}\right.$$
$$\left.+\frac{x_0g_{2a+}+x_2g_{a+}}{(x_0^2+g_{a+}^2)(x_2^2+g_{2a+}^2)}-\frac{4xg_{a+}}{(x^2+g_{a+}^2)^2}\right]-\frac{\Omega_{p0}^2}{4\pi}\frac{sa}{\pi}\int_{-\infty}^{0}\frac{dx}{\omega}\left\{\frac{(x_0-x_2)(a^2+x_0^2-g_0^2)-2x_0g_0(g_0+g_2)}{[(x_0-x_2)^2+(g_0+g_2)^2][(a^2+x_0^2-g_0^2)^2+4x_0^2g_0^2]}\right.$$
$$\left.-\frac{(x_1-x_0)(a^2+x_1^2-g_1^2)-2x_1g_1(g_0+g_1)}{[(x_1-x_0)^2+(g_0+g_1)^2][(a^2+x_1^2-g_1^2)^2+4x_1^2g_1^2]}\right\},\tag{B4}$$

with $x_0=x-\Sigma_1(x)$, $x_1=x+\omega-\Sigma_1(x+\omega)$, $x_2=x-\omega-\Sigma_1(x-\omega)$, $g_0=g(x)$, $g_1=g(x+\omega)$, $g_2=g(x-\omega)$, $g_{a\pm}=g_0\pm a$, $g_{1a\pm}=g_1\pm a$, and $g_{2a\pm}=g_2\pm a$.

[1] A.V. Puchkov, D.N. Basov, and T. Timusk, J. Phys.: Condens. Matter **8**, 10049 (1996).
[2] T. Timusk and B. Statt, Rep. Prog. Phys. **62**, 61 (1999).
[3] C.M. Varma, Int. J. Mod. Phys. B **3**, 2083 (1989).
[4] C.M. Varma, P.B. Littlewood, S. Schmitt-Rink, E. Abrahams, and A.E. Ruckenstein, Phys. Rev. Lett. **63**, 1996 (1989); **64**, 497 (1990).
[5] E. Abrahams and C.M. Varma, Proc. Natl. Acad. Sci. U.S.A. **97**, 5714 (2000).
[6] F. Marsiglio and J.P. Carbotte, Aust. J. Phys. **50**, 975 (1997).
[7] F. Marsiglio and J.P. Carbotte, Aust. J. Phys. **50**, 1011 (1997).
[8] R.E. Walstedt, W.W. Warren, Jr., R.F. Bell, R.J. Cava, G.P. Espinosa, L.F. Schneemeyer, and J.V. Waszczak, Phys. Rev. B **41**, 9574 (1990).
[9] W.W. Warren, Jr., R.E. Walstedt, G.F. Brennert, R.J. Cava, R. Tycko, R.F. Bell, and G. Dabbagh, Phys. Rev. Lett. **62**, 1193 (1989).
[10] H. Takagi, B. Batlogg, H.L. Kao, J. Kwo, R.J. Cava, J.J. Krajewski, and W.F. Peck, Jr., Phys. Rev. Lett. **69**, 2975 (1992).
[11] T. Ito, K. Takenaka, and S. Uchida, Phys. Rev. Lett. **70**, 3995 (1993).
[12] J.W. Loram, K.A. Mirza, J.R. Cooper, and W.Y. Liang, J. Supercond. **7**, 243 (1994).
[13] J.W. Loram, K.A. Mirza, J.R. Cooper, and J.L. Tallon, Physica C **282-287**, 1405 (1997).
[14] J. W. Loram, K. A. Mirza, J. R. Cooper, N. Athanassopoulou, and W. Y. Liang, in *Proceedings of the 10th HTC Anniversary Workshop on Physics, Materials and Applications*, edited by B. Batlogg, *et al.* (World Scientific, Singapore, 1996), p. 341.
[15] C.C. Homes, T. Timusk, R. Liang, D.A. Bonn, and W.N. Hardy, Phys. Rev. Lett. **71**, 1645 (1993).
[16] Ch. Renner, B. Revaz, J.-Y. Genoud, K. Kadowaki, and O. Fischer, Phys. Rev. Lett. **80**, 149 (1998).
[17] A.G. Loeser, Z.X. Shen, D.S. Dessau, D.S. Marshall, C.H. Park, P. Fournier, and A. Kapitulnik, Science **273**, 325 (1996).
[18] H. Ding, T. Yobaya, J.C. Campuzano, T. Takahashi, M. Randeria, M.R. Norman, T. Mochiku, K. Kadowaki, and J. Giapinzakis, Nature (London) **382**, 51 (1996).
[19] J.M. Harris, Z.-X. Shen, P.J. White, D.S. Marshall, M.C. Schabel, J.N. Eckstein, and I. Bozovic, Phys. Rev. B **54**, 15 665 (1996).
[20] P.W. Anderson, Science **235**, 1196 (1987).
[21] P.A. Lee and N. Nagaosa, Phys. Rev. B **46**, 5621 (1992).
[22] P.A. Lee and X.G. Wen, Phys. Rev. Lett. **78**, 4111 (1997).
[23] V.J. Emery, S.A. Kivelson, and O. Zachar, Phys. Rev. B **56**, 6120 (1997).
[24] V.J. Emery and S.A. Kivelson, Nature (London) **374**, 434 (1995).
[25] Qijin Chen, Ioan Kosztin, Boldizsár Jankó, and K. Levin, Phys. Rev. Lett. **81**, 4708 (1998).
[26] S. Chakravarty, R.B. Laughlin, D.K. Morr, and C. Nayak, Phys. Rev. B **63**, 094503 (2001).
[27] F. Marsiglio, J.P. Carbotte, and E. Schachinger, Phys. Rev. B **65**, 014515 (2002).
[28] D.N. Basov, E.J. Singley, and S.V. Dordevic, Phys. Rev. B **65**, 054516 (2002).
[29] G. D. Mahan, *Many-Particle Physics* (Plenum Press, New York, 1993).
[30] B. M. Klein, D. A. Papaconstantopoulos, and L. L. Boyer, in *Superconductivity in d- and f-Band Metals*, edited by H. Suhl and M. B. Maple (Academic Press, New York, 1980), p. 455.
[31] P. Horsch and H. Rietschel, Z. Phys. B **27**, 153 (1977).
[32] S.J. Nettel and H. Thomas, Solid State Commun. **21**, 683 (1977).
[33] S.G. Lie and J.P. Carbotte, Solid State Commun. **26**, 511 (1978).
[34] M. Weger and I. B. Goldberg, in *Solid State Physics*, edited by M. Ehrenreich, F. Seitz, and D. Turnbull (Academic Press, New York, 1973), Vol. 28, p. 1.
[35] W.E. Pickett, Phys. Rev. B **21**, 3897 (1980).
[36] B. Mitrović and J.P. Carbotte, Can. J. Phys. **61**, 758 (1983); **61**, 784 (1983); **61**, 872 (1983).
[37] B. Mitrović, Ph.D thesis, McMaster University, 1981.
[38] As an explicit example near a van Hove singularity in $N(\epsilon)$, the Fermi velocity becomes small and the product $N(\epsilon)v(\epsilon)^2$ goes like $v(\epsilon)$ which is small.